

# Pre-trained Models Perform the Best When Token Distributions Follow Zipf’s Law

Anonymous ACL submission

## Abstract

Tokenization is a fundamental step in natural language processing (NLP) and other sequence modeling domains, where the choice of vocabulary size significantly impacts model performance. Despite its importance, selecting an optimal vocabulary size remains underexplored, typically relying on heuristics or dataset-specific choices. In this work, we propose a principled method for determining the vocabulary size by analyzing token frequency distributions through Zipf’s law. We show that downstream task performance correlates with how closely token distributions follow power-law behavior, and that aligning with Zipfian scaling improves both model efficiency and effectiveness. Extensive experiments across NLP, genomics, and chemistry demonstrate that models consistently achieve peak performance when the token distribution closely adheres to Zipf’s law, establishing Zipfian alignment as a robust and generalizable criterion for vocabulary size selection.

## 1 Introduction

Tokenization is a fundamental preprocessing step in natural language processing (NLP), where raw text is segmented into smaller units known as tokens (Sennrich et al., 2016). These tokens can represent words, subwords, or characters, depending on the tokenization strategy (Schuster and Nakajima, 2012), and they form the basis for subsequent representation learning. The choice of tokenizer and its vocabulary size has a direct impact on model capacity, robustness, and computational efficiency (Devlin et al., 2019).

Among various strategies, Byte Pair Encoding (BPE) (Sennrich et al., 2016) is the most widely adopted method in modern large language models. Existing large language models typically fix a vocabulary size (e.g., 50K) (Achiam et al., 2023) in advance, then apply BPE to construct the tokenizer. This fixed-size approach, while convenient, lacks

a principled basis and may not be optimal across different tasks, domains, or languages.

In practice, choosing too small a vocabulary may lead to fragmented or overly fine-grained tokens, resulting in longer sequences and degraded semantic representation (Provilkov et al., 2020). On the other hand, overly large vocabularies may introduce redundancy, inflate memory usage, and reduce model efficiency (Brown et al., 2020). However, vocabulary size is often treated as a fixed hyperparameter, determined heuristically or based on dataset statistics (Kudo and Richardson, 2018).

Several prior works have explored metrics such as fertility (token-per-word ratio), parity (cross-lingual symmetry), and coverage to evaluate tokenizers (Liu et al., 2020; Wu et al., 2016). However, these metrics have been shown to correlate poorly with downstream task performance (Ali et al., 2024), especially when moving beyond NLP to other modalities such as genomics or chemistry. As a result, there remains a need for a more robust criterion to guide vocabulary size selection.

In this work, we propose a principled approach inspired by Zipf’s law, a well-known linguistic phenomenon whereby word frequency is inversely proportional to its rank in natural language corpora (Powers, 1998). We hypothesize that effective tokenizers should induce token frequency distributions that align with Zipfian behavior. To test this hypothesis, we introduce the *Zipf alignment score*, which quantifies how closely a tokenizer’s frequency distribution fits a power-law on a log-log plot. We use this score as a proxy metric to guide vocabulary size selection.

Empirically, we demonstrate that token distributions adhering more closely to Zipf’s law correspond to better downstream performance. Our experiments span NLP, genomics, and chemistry tasks, showing that Zipf alignment consistently predicts optimal vocabulary size across modalities.

To summarize, the main contributions of our

084 paper are as follows:  
 085 • We show that as the vocabulary size increases, the  
 086 token frequency distribution on a log-log scale  
 087 becomes increasingly linear, reflecting stronger  
 088 alignment with Zipf’s law.  
 089 • We demonstrate that downstream task perfor-  
 090 mance consistently improves and reaches its peak  
 091 when the token distribution most closely follows  
 092 Zipfian behavior.  
 093 • We propose a principled approach for selecting  
 094 vocabulary size by measuring the degree of Zipf  
 095 alignment in the token distribution. This method  
 096 is simple, generalizable across domains, and pre-  
 097 dictive of optimal performance.

## 098 2 Related Work

099 **Tokenization** Tokenization, the process of seg-  
 100 menting raw data into smaller units, is a critical  
 101 step in NLP and other fields. Classic methods like  
 102 BPE (Sennrich et al., 2016) and WordPiece (Schus-  
 103 ter and Nakajima, 2012) use subword segmentation  
 104 to balance vocabulary size and out-of-vocabulary  
 105 handling, while SentencePiece (Kudo and Richard-  
 106 son, 2018) enables language-independent tokeniza-  
 107 tion. These methods are foundational for modern  
 108 models like BERT (Devlin et al., 2019) and GPT  
 109 (Radford et al., 2019), as tokenization directly im-  
 110 pacts model efficiency, robustness, and downstream  
 111 task performance. Beyond text, tokenization has  
 112 been adapted for genomics (e.g., k-mer tokeniza-  
 113 tion in DNABERT (Ji et al., 2021)), chemistry (e.g.,  
 114 SMILES segmentation (Schwaller et al., 2019)),  
 115 and even vision and audio, where images are split  
 116 into patches and audio into spectrograms (Dosovit-  
 117 skiy et al., 2021; Radford et al., 2023), demonstrat-  
 118 ing its versatility across modalities.

119 **Tokenizer Selection Criteria** Prior work has ex-  
 120 plored several heuristics for selecting tokenizers.  
 121 One common approach is to use compression ra-  
 122 tio as a proxy, under the assumption that better  
 123 compression implies more efficient representations.  
 124 Goldman et al. (2024) examine this hypothesis and  
 125 find that compression correlates with performance  
 126 in some cases, but not consistently. Ali et al. (2024)  
 127 further evaluate metrics such as fertility, parity, and  
 128 compression, showing that these do not reliably pre-  
 129 dict downstream task performance. These findings  
 130 suggest that standard metrics often fail to capture  
 131 what makes a tokenizer effective, highlighting the  
 132 need for more robust, task-aware criteria.

**Zipf’s law and Power Law** Power-law distribu-  
 tions were first studied by Pareto in the context  
 of wealth distribution (Pareto, 1964). Zipf later  
 formalized this phenomenon in linguistics, show-  
 ing that word frequencies in natural language fol-  
 low a power-law distribution, now known as Zipf’s  
 law (Zipf, 2013). This distribution reveals that  
 a small number of words dominate the text fre-  
 quency, while most words are uncommon, a pat-  
 tern that is consistent across languages and corpora  
 (Montemurro, 2001). Power-law distributions are  
 also prevalent in other domains, including biology,  
 where gene expression levels and protein networks  
 exhibit scaling laws (Jeong et al., 2001), and in  
 social networks, where the degree distribution of  
 connections follows power-law behavior (Barabási  
 and Albert, 1999).

## 3 Observing Zipf’s Law

One of the most widely adopted subword tokeniza-  
 tion methods is Byte Pair Encoding (BPE) (Gage,  
 1994), which iteratively merges the most frequent  
 adjacent character pairs in a corpus until a prede-  
 fined vocabulary size is reached. The BPE algo-  
 rithm is shown in Appendix A. BPE has been  
 extensively used in state-of-the-art large-scale lan-  
 guage models. Given its widespread adoption, BPE  
 shows its importance in NLP research.

### 3.1 Vocabulary Size

Vocabulary size is a critical yet often overlooked  
 factor in designing tokenizers. If a model is trained  
 on an infinitely large dataset that comprehensively  
 represents all knowledge, and if the model has ac-  
 cess to unlimited computational resources, then  
 vocabulary size is of minimal concern—one can  
 simply choose a sufficiently large vocabulary. How-  
 ever, in real-world scenarios, training datasets rep-  
 resent only a subset of global knowledge, and com-  
 putational resources impose practical limitations on  
 training. This makes vocabulary size an essential  
 hyperparameter.

A small vocabulary set may fail to capture the  
 fundamental characters of a dataset, leading to  
 excessive fragmentation of words and loss of se-  
 mantic information. Conversely, an overly large  
 vocabulary set would introduce redundancy, lead-  
 ing to inefficient token representations that are not  
 optimally compact. This trade-off is especially  
 pronounced when dealing with domain-specific  
 datasets, where suboptimal vocabulary choices can

182 significantly impact model performance.

183 Despite its importance, vocabulary size is often  
184 determined based on heuristics or set arbitrarily  
185 large without systematic optimization. Such arbitrary  
186 choices may prevent models from capturing  
187 the most meaningful token distributions for a given  
188 dataset, potentially limiting performance. We argue  
189 that optimal vocabulary size should be carefully de-  
190 termined for each dataset, particularly in different  
191 modalities such as NLP, genomics, and chemistry.  
192 Identifying the appropriate vocabulary size for a  
193 given domain is crucial for maximizing informa-  
194 tion retention and model efficiency.

### 195 3.2 Power Law and Token Rank-Frequency 196 Distributions

197 Power law distributions characterize many natu-  
198 rally occurring phenomena, including linguistic  
199 structures. A power law describes a relationship  
200 where the frequency of an event is inversely pro-  
201 portional to its rank, typically expressed as  $f(x) \propto$   
202  $x^{-k}$ , where  $x$  is the rank (Pareto, 1964).

203 The log-log token rank-frequency distribution  
204 is based on empirical observations of textual data  
205 and is used to analyze the probabilistic structure  
206 of word frequencies within a text or corpus. In  
207 this representation, both the frequency of tokens  
208 (words) and their rank by frequency are plotted  
209 on logarithmic scales. If the token frequency fol-  
210 lows a perfect power-law distribution, the plot  
211 should form a straight line. However, in many real-  
212 world datasets, as shown in Section 5 and Figure 1,  
213 the plot often consists of segments with different  
214 slopes, indicating the presence of multiple classes  
215 of tokens with varying degrees of redundancy.

216 In natural language, we typically observe that  
217 vocabulary distributions follow a power-law when  
218 trained on sufficiently large datasets. This obser-  
219 vation motivates us to investigate token distribu-  
220 tion patterns, particularly in specific datasets or do-  
221 mains. It leads us to ask: *What is the optimal token*  
222 *distribution for a given domain or dataset? Can*  
223 *we determine the vocabulary size prior to training*  
224 *to obtain such an optimal distribution?*

### 225 3.3 Hypotheses and Vocabulary Size Selection 226 Strategy

227 Our study begins with the empirical observation  
228 that the *token rank-frequency distribution* exhibits  
229 a Zipfian pattern. This leads us to propose two hy-  
230 potheses that guide our vocabulary size selection:

- 231 1. **Hypothesis 1:** As vocabulary size increases,  
232 the log-log rank-frequency distribution of to-  
233kens gradually approaches a straight line, in-  
234dicating alignment with Zipf’s law.
- 235 2. **Hypothesis 2:** When the token distribu-  
236tion closely matches Zipf’s law, the model  
237 achieves superior downstream performance.

238 In this section, we focus on verifying **Hypothese-  
239sis 1** using the BookCorpus dataset. We train BPE-  
240based tokenizers with various vocabulary sizes  
241 (ranging from 2K to 50K) and visualize the result-  
242ing rank-frequency distributions in log-log space.

243 From Figure 1, we observe the following note-  
244worthy phenomenon:

245 **Observation 1:** When the vocabulary is small,  
246 the log-log rank-frequency distribution exhibits a  
247 clear curvature, deviating significantly from the  
248 ideal power-law form. As the vocabulary increases,  
249 the curve straightens and approximates a linear  
250 trend. This indicates that expanding vocabulary  
251 promotes statistical self-organization of token us-  
252 age, making the token distribution conform more  
253 closely to Zipf’s law. This observation directly sup-  
254 ports **Hypothesis 1**, showing that Zipfian behavior  
255 emerges naturally as the vocabulary grows. Moti-  
256 vated by this, we design a data-driven vocabulary  
257 selection strategy that leverages Zipfian alignment  
258 as a stopping criterion for vocabulary expansion.

259 To automatically determine an appropriate vo-  
260cabulary size, we design an iterative algorithm that  
261 gradually grows the vocabulary and monitors how  
262 well the resulting token distribution aligns with  
263 Zipf’s law. The alignment is quantified using a  
264 statistical goodness-of-fit score, such as the coef-  
265 ficient of determination ( $R^2$ ), computed between  
266 the empirical log-log rank-frequency curve and an  
267 ideal Zipfian distribution.

268 The procedure begins with a small initial vocabu-  
269lary and expands it step by step using BPE or a  
270 similar merge-based algorithm. After the  $t$ -th up-  
271 date of vocabulary, we re-tokenize the corpus and  
272 calculate the new Zipfian fit score, denoted as  $\text{Zipf}_t$ .  
273 We keep track of the best Zipf score  $\text{Zipf}_{\max}$ .

274 To determine when the vocabulary has grown  
275 sufficiently, we introduce a stagnation counter that  
276 monitors whether further merges lead to meaning-  
277 ful improvements in Zipfian alignment. Specifi-  
278 cally, if the score  $\text{Zipf}_t$  fails to exceed  $\text{Zipf}_{\max}$   
279 by more than a small threshold  $\epsilon$  after  $N$  steps,  
280 we consider the Zipfian fit to have stabilized. At  
281 this point, the vocabulary is no longer expanded,  
282 and the current vocabulary is taken as the optimal set,

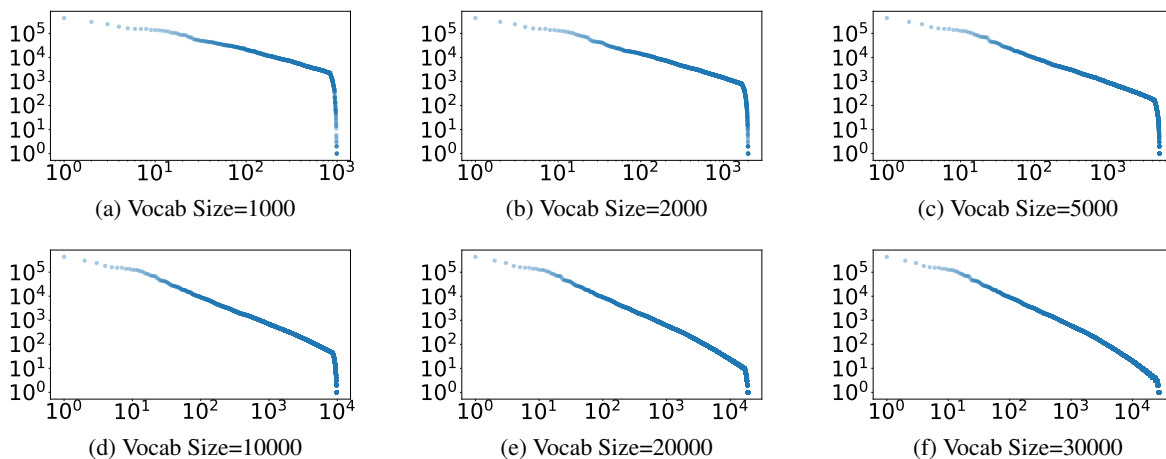


Figure 1: Log-log rank-frequency distribution of different vocabulary sizes on BookCorpus. As the size increases, the curves become increasingly linear, indicating closer adherence to Zipf’s law.

denoted by  $\mathcal{V}_{\text{opt}}$ .

This method adapts vocabulary size to the statistical structure of the data and does not rely on arbitrary preset vocabulary sizes. In Section 5, we evaluate **Hypothesis 2** and analyze how Zipfian alignment correlates with downstream task performance across different modalities.

## 4 Method

### 4.1 Models and Pre-training Methods

We conduct experiments across multiple domains, including NLP, genomics (Gene), and chemistry (Chem), to evaluate the impact of vocabulary size on model performance. For each domain, we follow a two-stage process: pre-training on domain-specific datasets and fine-tuning on downstream tasks. In the NLP domain, both encoder-only model (e.g., BERT (Devlin et al., 2019)) and encoder-decoder model (e.g., mBART (Liu et al., 2020)) are evaluated. For BERT, we pre-train the model on a combination of OpenWebText (Gokaslan and Cohen, 2019) and BookCorpus (Zhu et al., 2015) datasets, following the standard Masked Language Modeling (MLM) objective (Devlin et al., 2019). The pre-trained BERT model is then fine-tuned on the GLUE benchmark, which includes tasks such as sentiment analysis, textual entailment, and paraphrase detection, and the model performance is evaluated using the GLUE score (Wang et al., 2018).

For mBART, we pre-train the model on the WMT dataset using the Multilingual Denoising Pre-training objective, focusing on three language pairs: German-English (De-En), French-English (Fr-En), and Chinese-English (Zh-En) (Liu et al.,

2020). The pre-trained mBART model is fine-tuned on downstream translation tasks for the respective language pairs and the performance is evaluated using the BLEU score (Papineni et al., 2002).

In the genomics domain, we follow the approach of DNABERT2 (Zhou et al., 2024), using a BERT-based architecture tailored for DNA sequences. We pre-train the model on DNA sequences from the same dataset used in DNABERT2, employing the MLM objective. Fine-tuning is performed on downstream classification tasks such as promoter prediction and splice site detection, with model performance evaluated using accuracy.

In the chemistry domain, we focus on the SMILES representation of molecular structures, using a BERT-based architecture. We pre-train the model on the first 5 million data in ZINC20, a large dataset of SMILES sequences representing chemical compounds (Irwin and Shoichet, 2005). Fine-tuning is performed on downstream classification tasks such as molecular property prediction, and performance is evaluated using the ROC-AUC score.

### 4.2 Insight for Bigger Models

Due to resource constraints, we are limited to fine-tuning relatively smaller models. However, Ruder et al. (2019) argue that fine-tuning a smaller pre-trained model on a smaller dataset can yield competitive results compared to training a large model from scratch, particularly for specific domains or tasks. Based on this perspective, the conclusions drawn from our experiments on smaller models can also be extended to larger models, offering valuable insights for scaling up model architectures.

### 4.3 Finetuning Dataset and Evaluation Metrics

For NLP tasks, we fine-tune BERT on the GLUE benchmark, excluding the WNLI task (Wang et al., 2018). The selected tasks and their evaluation metrics are as follows: CoLA uses the Matthews correlation coefficient (MCC); MRPC and QQP use the average of accuracy and F1 score; STS-B uses the average of Pearson and Spearman correlation; and the remaining tasks are evaluated using accuracy.

For NLP tasks with the mBART model, the model is first pre-trained on the WMT dataset (Bojar et al., 2016) for each language pair, and then fine-tuned on the IWSLT dataset, specifically: IWSLT14(Cettolo et al., 2014) for De-En, IWSLT17(Cettolo et al., 2017) for Fr-En, and IWSLT15(Cettolo et al., 2015) for Zh-En.

For genomics tasks with BERT, we use the GUE dataset that has 4 tasks: Core Promoter Detection, Transcription Factor Prediction, Promoter Detection, and Epigenetic Marks Prediction.

For the chemistry tasks with BERT, we use the MoleculeNet dataset, specifically the BBBP, Tox21, Sider, ClinTox, HIV, and BACE datasets, and use ROC-AUC as the evaluation metric .

### 4.4 Determining Vocabulary Size

Determining vocabulary size is crucial for downstream tasks, as different domains require varying levels of token granularity. For NLP tasks, experiments are conducted with BERT vocabulary sizes ranging from 2,000 to 50,000. For multilingual translation tasks, vocab sizes between 2,000 and 140,000 are utilized, as both languages share a common tokenizer. In the genomics and chemistry domains, where the character set is limited, vocab sizes between 500 and 8,000 are employed. This experimental setup enables a systematic analysis of the influence of vocabulary size on model effectiveness across these diverse modalities, providing insights into the optimal tokenizer configurations required for different types of data.

## 5 Experiment Results

Building on the empirical foundation established in Section 3.3, we now turn to validating **Hypothesis 2**: that model performance improves when the token rank-frequency distribution closely follows Zipf’s law. While Section 3.3 demonstrated the natural emergence of Zipfian behavior with increasing vocabulary size, this section investigates whether

such statistical alignment correlates with improvements in downstream task performance.

To this end, we evaluate the impact of vocabulary size across multiple domains—including **natural language**, **genomics**, and **chemistry**—to test whether Zipfian alignment provides a meaningful criterion for optimizing tokenizer vocabulary. We analyze:

- The relationship between Zipfian goodness-of-fit (measured via  $R^2$ ) and model performance;
- How the optimal vocabulary size varies across domains;
- Whether alignment with Zipf’s law generalizes beyond NLP to other modalities;
- Case studies and ablations to validate the robustness of our observations.

This analysis provides strong empirical support for using Zipfian properties as an automatic, interpretable, and domain-agnostic guide for vocabulary size selection.

### 5.1 Impact on NLP task performance

To quantify the impact of vocabulary size, we evaluate BERT-Medium models trained with different vocabulary sizes on the GLUE benchmark, covering eight NLP tasks. The results in Table 1 indicate that models trained with 30,000 vocabulary size consistently achieve the highest performance. Notably, performance at 30,000 is significantly higher than at smaller vocabulary sizes, while further increasing vocabulary size to 35,000 or 50,000 yields marginal or even slightly worse results.

To better illustrate this trend, Figure 2a presents the task performance as a function of vocabulary size. The curve exhibits a clear upward trajectory, peaking at 30,000 before plateauing. Cancho and Solé (2001) empirically demonstrated that word-frequency distributions in large corpora exhibit two distinct power-law regimes, with clear inflection points in the exponent values. This observation motivates the application of segmented fitting and enables a quantitative evaluation of linearity on log-log rank-frequency plots. Alternative validation methods for power-law behavior include maximum-likelihood estimation combined with goodness-of-fit tests based on the Kolmogorov-Smirnov statistic, which measures the greatest vertical deviation between empirical and theoretical cumulative distributions (Clauset et al., 2009). The Kolmogorov-Smirnov statistic, however, is notably insensitive to variations in the distribution tails, where the most significant power law behavior arises. While pro-

Vocab size	CoLA Matthews	SST-2 Acc.	MRPC Acc./F1	STS-B Cor.	QQP Acc./F1	MNLI Acc.	QNLI Acc.	RTE Acc.	Avg	$R^2$
2,000	24.83	84.64	77.49	78.46	84.63	69.74	77.31	63.52	70.08	0.6939
5,000	28.87	86.07	78.41	79.42	85.78	72.03	80.71	64.22	71.94	0.7735
10,000	36.02	88.78	82.54	83.62	87.37	79.01	86.25	64.57	76.02	0.8340
20,000	44.22	91.61	84.33	86.79	88.92	81.42	87.74	67.32	79.04	0.8911
25,000	49.73	91.25	85.63	86.82	88.97	82.03	87.91	67.54	79.99	0.9119
27,500	51.79	91.84	86.02	87.14	89.25	82.21	88.34	67.89	80.56	0.9198
30,000	<b>54.92</b>	92.36	86.37	<b>87.45</b>	89.52	<b>82.52</b>	<b>88.96</b>	<b>68.94</b>	<b>81.38</b>	0.9372
32,500	52.37	<b>92.42</b>	86.30	87.32	<b>89.78</b>	82.31	88.63	68.53	80.96	0.9344
35,000	53.64	92.39	<b>86.42</b>	87.42	89.63	82.51	88.72	68.76	81.19	0.9397
37,500	52.97	92.47	86.29	87.21	89.54	82.34	88.52	68.69	81.00	0.9408
40,000	53.27	92.21	86.24	87.37	89.31	82.29	88.65	68.42	80.97	0.9425
50,000	50.23	91.83	85.95	86.47	88.88	81.94	88.26	67.94	80.19	0.9414

Table 1: Performance comparison across various classification tasks. Metrics are accuracy for SST-2, MNLI, QNLI and RTE; Matthews correlation for CoLA; the average of accuracy and F1 scores for MRPC and QQP; and the average of Pearson and Spearman correlations for STS-B. Each configuration is run three times with different random seeds, and the averaged results are taken as the final performance.

451 viding a more comprehensive assessment by assign- 484  
452 ing additional weight to tail differences, metrics 485  
453 such as the Kuiper or Anderson-Darling statistics 486  
454 introduce added complexity to the analysis(Clauset 487  
455 et al., 2009). Given the dual-regime structure ob- 488  
456 served in Figure 1 and the importance of accurately 489  
457 capturing both the head and the tail of Zipfian dis- 490  
458 tributions, we approximate each rank-frequency 491  
459 distribution with a least squares linear fit and adopt 492  
460 the coefficient of determination  $R^2$  as goodness- 493  
461 of-fit measure because it offers an intuitive and 494  
462 interpretable quantification of linearity across the 495  
463 entire rank-frequency spectrum. 496

464 The results show that as vocabulary size in- 497  
465 creases, the  $R^2$  value steadily improves. Specif- 498  
466 ically, before reaching a vocabulary size of 30,000, 499  
467 the  $R^2$  value increases rapidly, while after reach- 500  
468 ing 30,000, the  $R^2$  value stabilizes at a high value. 501  
469 From Figure 2a, we observe that  $R^2$  closely follows 502  
470 the trend of the average performance. This further 503  
471 demonstrates that the closeness to Zipf’s law at 504  
472 different vocabulary sizes reflects the performance 505  
473 of downstream tasks. 506

474 Similar conclusions can be drawn from the re- 507  
475 sults of the translation tasks (Table 4 in Appendix 508  
476 B). When the  $R^2$  metric reaches its optimal value, 509  
477 the BLEU score is also relatively high. Figure 2d 510  
478 illustrates the relationship between the translation 511  
479 task performance and vocabulary size for three lan- 512  
480 guage pairs. Obviously, the trend of  $R^2$  is consis- 513  
481 tent with the task performance. 514

482 **Observation 2:** The token rank-frequency distri- 515  
483 bution can serve as a prior indicator of a pre-trained 516

model’s performance on downstream tasks. When 484  
the token distribution approaches a power law, it 485  
suggests that the tokenizer is well-suited for the 486  
task, leading to better performance on downstream 487  
tasks. This suggests that closeness to Zipf’s law 488  
can be a useful metric for choosing the best tok- 489  
enizer and vocabulary. 490

## 5.2 Generalization to Genomics and Chemistry 491

To assess its generalizability, the proposed ap- 493  
proach is extended to genomics and chemistry, 494  
where determining the vocabulary remains an open 495  
challenge. 496

In genomics, we pre-train BERT-based mod- 497  
els on DNA sequences, following the setup of 498  
DNABERT2, and evaluate performance on vari- 499  
ous GUE classification tasks. The results presented 500  
in Table 2 indicate that optimal performance is 501  
achieved with moderate vocabulary sizes, specif- 502  
ically around 4000. Notably, for 5 out of the 503  
8 tasks, the BERT model trained with a 4000- 504  
vocabulary-size tokenizer demonstrates superior 505  
accuracy scores. As shown in Figure 2c, the  $R^2$  506  
value continues to rise as the vocabulary size in- 507  
creases up to 4000, after which there is no signifi- 508  
cant improvement. This aligns with our intuition: 509  
smaller vocabularies fail to capture biologically 510  
meaningful substructures, while excessively large 511  
vocabularies lead to redundant segmentations. 512

Similarly, in chemistry, we tokenize SMILES 513  
molecular representations and pre-train models us- 514  
ing the ZINC20 dataset. The results presented in 515  
Table 3 indicate that performance continues to im- 516

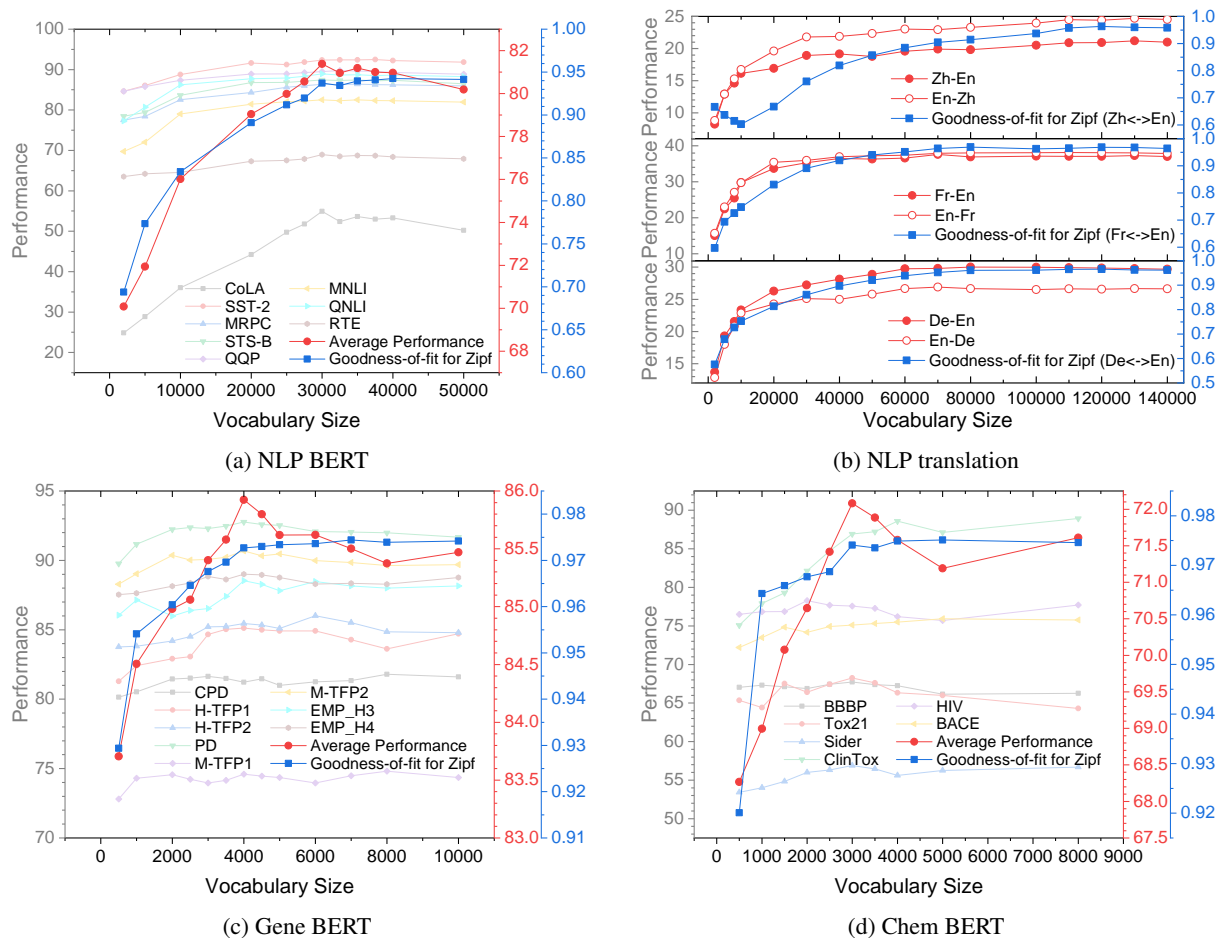


Figure 2: Model performance with different vocabulary sizes across four distinct domains. Model performance exhibits a consistent trend with the Zipfian goodness-of-fit

517 prove as vocabulary size increases from 500 to  
 518 3000. However, after reaching a vocabulary size of  
 519 3000, performance begins to slightly decline with  
 520 further increases in vocabulary size. A vocabulary  
 521 size of 3000 yields the best performance, achiev-  
 522 ing the highest ROC-AUC score and the highest  
 523 average score. By examining the  $R^2$  metric in both  
 524 Table 3 and Figure 2d, we observe that a vocabu-  
 525 lary size of 3000 represents the turning point. This  
 526 finding further supports our Observation 2 in the  
 527 chemistry domain and provides valuable insight  
 528 for utilizing an appropriate tokenizer that can ef-  
 529 fectively capture functional groups in molecular  
 530 structures.

### 5.3 Case Studies: Tokenization Granularity Across Vocabulary Sizes

531 In the case studies section, we provide examples to  
 532 show that having a vocabulary that is too small or  
 533 too large is not appropriate. The figure shows ex-  
 534 amples from both the NLP and chemistry domains  
 535 to illustrate this conclusion.  
 536  
 537

538 In the first example below, we do analysis for  
 539 CCC0c1ccc(cc1)c2cccc3c2nccn3 – the SMILES  
 540 representation of the molecule, and compare how  
 541 different vocabulary sizes affect its tokenization.  
 542 With a small vocabulary size, the molecule is overly  
 543 fragmented—for instance, into tokens like c1ccc  
 544 and ccn3(cc1)—which breaks apart chemically  
 545 meaningful structures and leads to unstable or un-  
 546 interpretable fragments. At an appropriate vocabu-  
 547 lary size, the tokenizer produces segments such as  
 548 CCC0c1ccc, (cc1), and c2cccc3c2, which aligns  
 549 with functional groups and aromatic or heterocyclic  
 550 rings, enhancing chemical interpretability. How-  
 551 ever, when the vocabulary is too large, tokens like  
 552 c2cccc3c2n emerge, which over-merge frequent  
 553 but semantically inconsistent character sequences.  
 554 These tokens span across distinct substructures, dis-  
 555 rupting meaningful chemical units and weakening  
 556 the tokenizer’s ability to preserve domain-relevant  
 557 structure. This observation reinforces the impor-  
 558 tance of choosing a vocabulary size that balances  
 559 token compactness with chemical coherence.

Vocab size	CPD Acc.	H-TFP1 Acc.	H-TFP2 Acc.	PD Acc.	M-TFP1 Acc.	M-TFP2 Acc.	EMP_H3 Acc.	EMP_H4 Acc.	Avg	$R^2$
500	80.15	81.29	83.76	89.77	72.81	88.28	86.05	87.53	83.71	0.9294
1,000	80.53	82.42	83.81	91.16	74.31	89.03	87.14	87.64	84.51	0.9541
2,000	81.45	82.91	84.20	92.23	74.56	90.36	85.99	88.15	84.98	0.9604
2,500	81.52	83.07	84.51	92.37	74.23	90.02	86.39	88.37	85.06	0.9646
3,000	81.64	84.67	85.21	92.29	73.96	90.07	86.53	88.84	85.40	0.9676
3,500	81.49	85.03	85.24	92.47	74.15	90.22	87.41	88.62	85.58	0.9696
4,000	81.23	<b>85.12</b>	85.45	<b>92.76</b>	74.60	<b>90.68</b>	<b>88.54</b>	<b>89.01</b>	<b>85.92</b>	0.9727
4,500	81.46	84.99	85.34	92.59	74.46	90.33	88.27	88.95	85.80	0.9730
5,000	81.00	84.92	85.10	92.53	74.35	90.47	87.81	88.77	85.62	0.9734
6,000	81.25	84.92	<b>86.01</b>	92.08	73.96	89.99	88.47	88.29	85.62	0.9736
7,000	81.34	84.28	85.52	92.04	74.48	89.85	88.16	88.35	85.50	0.9744
8,000	<b>81.80</b>	83.62	84.85	91.99	<b>74.81</b>	89.63	88.01	88.28	85.37	0.9739
10,000	81.61	84.72	84.79	91.67	74.35	89.69	88.16	88.77	85.47	0.9742

Table 2: Performance comparison of different vocabulary sizes in gene-related classification tasks. Accuracy is reported for all tasks, measuring the performance of BERT-based models on DNA sequence classification. Each configuration is run three times with different random seeds, and the averaged results are reported.

Vocab size	BBBP ROC	Tox21 ROC	Sider ROC	ClinTox ROC	HIV ROC	BACE ROC	Avg ROC	$R^2$
500	67.05	65.34	53.41	75.09	76.51	72.20	68.27	0.9201
1,000	67.31	64.41	54.02	77.91	76.84	73.49	69.00	0.9643
1500	67.12	67.51	54.83	79.30	76.87	74.83	70.08	0.9659
2,000	66.89	66.39	56.00	82.14	<b>78.29</b>	74.17	70.65	0.9677
2,500	67.42	67.43	56.32	84.72	77.69	74.92	71.42	0.9687
3,000	<b>67.73</b>	<b>68.26</b>	<b>56.89</b>	86.92	77.58	75.11	<b>72.08</b>	0.9741
3,500	67.39	67.62	56.47	87.23	77.29	75.32	71.89	0.9735
4,000	67.24	66.34	55.61	<b>88.59</b>	76.20	75.50	71.58	0.9749
5,000	66.14	65.99	56.26	87.12	75.70	<b>75.93</b>	71.19	0.9751
8,000	66.27	64.29	56.69	88.94	77.71	75.77	71.61	0.9746

Table 3: Performance comparisons are performed on various classification tasks in the MoleculeNet dataset, using ROC-AUC scores as the evaluation metric. Each configuration is run three times with different random seeds, and the average is used as the final performance metric.

In the second example, we show how the phrase “invisible footprints” is tokenized with a vocabulary size of 30,000, correctly splitting it into “in” “visible” “foot” “prints”. When a smaller vocabulary size is used, the word is split into non-semantic tokens such as “in” “vis” “ible” “foot” “prin” “ts” resulting in a loss of semantic meaning. When the vocabulary size is too large, each word is treated as a single token, introducing semantic redundancy.

These examples further support our approach, providing insights into how vocabulary size influences tokenization quality and, in turn, impacts task performance. They reinforce our method that vocabulary size determining should be Zipfian-guided, ensuring that tokenization reflects intrinsic linguistic and structural patterns.

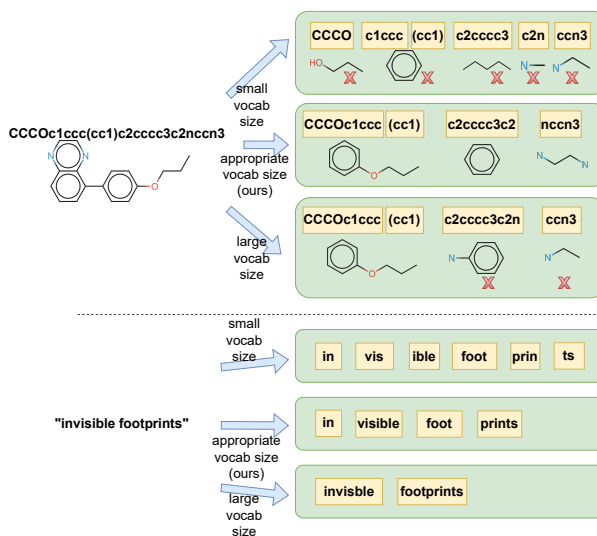


Figure 3: Case study: With an appropriate vocabulary size, the tokenization not only is more effective but also captures essential patterns of sequences.

## 6 Conclusion

This study explored the impact of tokenizer vocabulary size on the performance of pre-trained language models across various domains, including natural language processing, genomics, and chemistry. By analyzing the relationship between token rank-frequency distribution and task performance, we demonstrated that aligning token distributions with power-law scaling laws can serve as a robust criterion for determining optimal vocabulary sizes. Our experiments revealed that models achieve superior performance when the token distribution closely adheres to Zipf’s law, indicating that this alignment enhances both efficiency and effectiveness in downstream tasks.



## 7 Limitations

While our study provides valuable insights into the relationship between tokenizer vocabulary size and model performance, several limitations should be acknowledged.

Due to hardware limitations, we only conduct pre-training experiments on relatively small models. Although the conclusions drawn from these smaller models offer meaningful guidance for larger models, the significant difference in parameter scale means that our findings may not fully generalize to state-of-the-art architectures with billions of parameters. Further experiments on larger models are necessary to solidify our conclusions and validate the scalability of our approach.

Our experiments primarily focused on a subset of modalities (e.g., NLP, genomics, and chemistry) and a limited range of pre-trained model architectures (e.g., BERT and mBART). To further generalize our findings, future work should extend the evaluation to additional modalities (e.g., vision, audio) and diverse model architectures (e.g., Transformer variants, hybrid models).

## References

Josh Achiam, Steven Adler, Sandhini Agarwal, Lama Ahmad, Ilge Akkaya, Florencia Leoni Aleman, Diogo Almeida, Janko Altenschmidt, Sam Altman, Shyamal Anadkat, and 1 others. 2023. Gpt-4 technical report. *arXiv preprint arXiv:2303.08774*.

Mehdi Ali, Michael Fromm, Klaudia Thellmann, Richard Rutmann, Max Lübbering, Johannes Leveling, Katrin Klug, Jan Ebert, Niclas Doll, Jasper Buschhoff, and 1 others. 2024. Tokenizer choice for LLM training: Negligible or crucial? In *Findings of the Association for Computational Linguistics: NAACL 2024*, pages 3907–3924.

Albert-László Barabási and Réka Albert. 1999. Emergence of scaling in random networks. *science*, 286(5439):509–512.

Ondrej Bojar, Rajen Chatterjee, Christian Federmann, Yvette Graham, Barry Haddow, Matthias Huck, Antonio Jimeno Yepes, Philipp Koehn, Varvara Logacheva, Christof Monz, and 1 others. 2016. Findings of the 2016 conference on machine translation (WMT16). In *First conference on machine translation*, pages 131–198. Association for Computational Linguistics.

Tom Brown, Benjamin Mann, Nick Ryder, Melanie Subbiah, Jared D Kaplan, Prafulla Dhariwal, Arvind Neelakantan, Pranav Shyam, Girish Sastry, Amanda Askell, and 1 others. 2020. Language models are

few-shot learners. *Advances in neural information processing systems*, 33:1877–1901.

Ramon Ferrer Cancho and Ricard V. Solé. 2001. Two regimes in the frequency of words and the origins of complex lexicons: Zipf’s law revisited. *Journal of Quantitative Linguistics*, 8(3):165–173.

Mauro Cettolo, Marcello Federico, Luisa Bentivogli, Jan Niehues, Sebastian Stüker, Katsutho Sudoh, Koichiro Yoshino, and Christian Federmann. 2017. Overview of the iwslt 2017 evaluation campaign. In *Proceedings of the 14th International Workshop on Spoken Language Translation*, pages 2–14.

Mauro Cettolo, Jan Niehues, Sebastian Stüker, Luisa Bentivogli, Roldano Cattoni, and Marcello Federico. 2015. The IWSLT 2015 evaluation campaign. In *Proceedings of the 12th International Workshop on Spoken Language Translation: Evaluation Campaign*, pages 2–14, Da Nang, Vietnam.

Mauro Cettolo, Jan Niehues, Sebastian Stüker, Luisa Bentivogli, and Marcello Federico. 2014. Report on the 11th iwslt evaluation campaign. In *Proceedings of the 11th International Workshop on Spoken Language Translation: Evaluation Campaign*, pages 2–17.

Aaron Clauset, Cosma Rohilla Shalizi, and M. E. J. Newman. 2009. Power-law distributions in empirical data. *SIAM Review*, 51(4):661–703.

Jacob Devlin, Ming-Wei Chang, Kenton Lee, and Kristina Toutanova. 2019. BERT: Pre-training of deep bidirectional transformers for language understanding. In *Proceedings of the 2019 conference of the North American chapter of the association for computational linguistics: human language technologies, volume 1 (long and short papers)*, pages 4171–4186.

Alexey Dosovitskiy, Lucas Beyer, Alexander Kolesnikov, Dirk Weissenborn, Xiaohua Zhai, Thomas Unterthiner, Mostafa Dehghani, Matthias Minderer, Georg Heigold, Sylvain Gelly, Jakob Uszkoreit, and Neil Houlsby. 2021. An image is worth 16x16 words: Transformers for image recognition at scale. In *International Conference on Learning Representations*.

Philip Gage. 1994. A new algorithm for data compression. *The C Users Journal*, 12(2):23–38.

Aaron Gokaslan and Vanya Cohen. 2019. Openwebtext corpus. <https://skylion007.github.io/OpenWebTextCorpus/>. Accessed: 2024-05-20.

Omer Goldman, Avi Caciularu, Matan Eyal, Kris Cao, Idan Szpektor, and Reut Tsarfaty. 2024. Unpacking tokenization: Evaluating text compression and its correlation with model performance. In *Findings of the Association for Computational Linguistics: ACL 2024*, pages 2274–2286, Bangkok, Thailand. Association for Computational Linguistics.

697	John J Irwin and Brian K Shoichet. 2005. ZINC—a free database of commercially available compounds for virtual screening. <i>Journal of chemical information and modeling</i> , 45(1):177–182.	
698		
699		
700		
701	Hawoong Jeong, Sean P Mason, A-L Barabási, and Zoltan N Oltvai. 2001. Lethality and centrality in protein networks. <i>Nature</i> , 411(6833):41–42.	
702		
703		
704	Yanrong Ji, Zhihan Zhou, Han Liu, and Ramana V Davuluri. 2021. DNABERT: pre-trained bidirectional encoder representations from transformers model for DNA-language in genome. <i>Bioinformatics</i> , 37(15):2112–2120.	
705		
706		
707		
708		
709	Taku Kudo and John Richardson. 2018. <a href="#">SentencePiece: A simple and language independent subword tokenizer and detokenizer for neural text processing</a> . In <i>Proceedings of the 2018 Conference on Empirical Methods in Natural Language Processing: System Demonstrations</i> , pages 66–71, Brussels, Belgium. Association for Computational Linguistics.	
710		
711		
712		
713		
714		
715		
716	Yinhan Liu, Jiatao Gu, Naman Goyal, Xian Li, Sergey Edunov, Marjan Ghazvininejad, Mike Lewis, and Luke Zettlemoyer. 2020. <a href="#">Multilingual denoising pre-training for neural machine translation</a> . <i>Transactions of the Association for Computational Linguistics</i> , 8:726–742.	
717		
718		
719		
720		
721		
722	Marcelo A Montemurro. 2001. Beyond the Zipf–Mandelbrot law in quantitative linguistics. <i>Physica A: Statistical Mechanics and its Applications</i> , 300(3–4):567–578.	
723		
724		
725		
726	Kishore Papineni, Salim Roukos, Todd Ward, and Wei-Jing Zhu. 2002. <a href="#">BLEU: a method for automatic evaluation of machine translation</a> . In <i>Proceedings of the 40th Annual Meeting of the Association for Computational Linguistics</i> , pages 311–318, Philadelphia, Pennsylvania, USA. Association for Computational Linguistics.	
727		
728		
729		
730		
731		
732		
733	Vilfredo Pareto. 1964. <i>Cours d’économie politique</i> , volume 1. Librairie Droz.	
734		
735	David M. W. Powers. 1998. Applications and explanations of zipf’s law. In <i>Proceedings of the Joint Conferences on New Methods in Language Processing and Computational Natural Language Learning</i> , NeMLaP3/CoNLL ’98, page 151–160, USA. Association for Computational Linguistics.	
736		
737		
738		
739		
740		
741	Ivan Provilkov, Dmitrii Emelianenko, and Elena Voita. 2020. <a href="#">BPE-dropout: Simple and effective subword regularization</a> . In <i>Proceedings of the 58th Annual Meeting of the Association for Computational Linguistics</i> , pages 1882–1892, Online. Association for Computational Linguistics.	
742		
743		
744		
745		
746		
747	Alec Radford, Jong Wook Kim, Tao Xu, Greg Brockman, Christine McLeavey, and Ilya Sutskever. 2023. Robust speech recognition via large-scale weak supervision. In <i>Proceedings of the 40th International Conference on Machine Learning</i> , ICML’23. PMLR.	
748		
749		
750		
751		
	Alec Radford, Jeffrey Wu, Rewon Child, David Luan, Dario Amodei, Ilya Sutskever, and 1 others. 2019. Language models are unsupervised multitask learners. <i>OpenAI blog</i> .	752 753 754 755
	Sebastian Ruder, Matthew E. Peters, Swabha Swayamdipta, and Thomas Wolf. 2019. <a href="#">Transfer learning in natural language processing</a> . In <i>Proceedings of the 2019 Conference of the North American Chapter of the Association for Computational Linguistics: Tutorials</i> , pages 15–18, Minneapolis, Minnesota. Association for Computational Linguistics.	756 757 758 759 760 761 762 763
	Mike Schuster and Kaisuke Nakajima. 2012. <a href="#">Japanese and korean voice search</a> . In <i>2012 IEEE International Conference on Acoustics, Speech and Signal Processing (ICASSP)</i> , pages 5149–5152.	764 765 766 767
	Philippe Schwaller, Teodoro Laino, Théophile Gaudin, Peter Bolgar, Christopher A. Hunter, Costas Bekas, and Alpha A. Lee. 2019. <a href="#">Molecular transformer: A model for uncertainty-calibrated chemical reaction prediction</a> . <i>ACS Central Science</i> , 5(9):1572–1583.	768 769 770 771 772
	Rico Sennrich, Barry Haddow, and Alexandra Birch. 2016. <a href="#">Neural machine translation of rare words with subword units</a> . In <i>Proceedings of the 54th Annual Meeting of the Association for Computational Linguistics (Volume 1: Long Papers)</i> , pages 1715–1725, Berlin, Germany. Association for Computational Linguistics.	773 774 775 776 777 778 779
	Alex Wang, Amanpreet Singh, Julian Michael, Felix Hill, Omer Levy, and Samuel Bowman. 2018. <a href="#">GLUE: A multi-task benchmark and analysis platform for natural language understanding</a> . In <i>Proceedings of the 2018 EMNLP Workshop BlackboxNLP: Analyzing and Interpreting Neural Networks for NLP</i> , pages 353–355, Brussels, Belgium. Association for Computational Linguistics.	780 781 782 783 784 785 786 787
	Yonghui Wu, Mike Schuster, Zhifeng Chen, Quoc V Le, Mohammad Norouzi, Wolfgang Macherey, Maxim Krikun, Yuan Cao, Qin Gao, Klaus Macherey, and 1 others. 2016. Google’s neural machine translation system: Bridging the gap between human and machine translation. <i>arXiv preprint arXiv:1609.08144</i> .	788 789 790 791 792 793
	Zhihan Zhou, Yanrong Ji, Weijian Li, Pratik Dutta, Ramana V Davuluri, and Han Liu. 2024. <a href="#">DNABERT-2: Efficient foundation model and benchmark for multi-species genomes</a> . In <i>The Twelfth International Conference on Learning Representations</i> .	794 795 796 797 798
	Yukun Zhu, Ryan Kiros, Richard S Zemel, Ruslan Salakhutdinov, Raquel Urtasun, Antonio Torralba, and Sanja Fidler. 2015. Aligning books and movies: Towards story-like visual explanations by watching movies and reading books. In <i>Proceedings of the IEEE International Conference on Computer Vision (ICCV)</i> , pages 19–27.	799 800 801 802 803 804 805
	George Kingsley Zipf. 2013. <i>The psycho-biology of language: An introduction to dynamic philology</i> . Routledge.	806 807 808

Vocab size	De-En BLEU	En-De BLEU	$R^2$	Fr-En BLEU	En-Fr BLEU	$R^2$	Zh-En BLEU	En-Zh BLEU	$R^2$
2,000	13.67	12.83	0.5755	15.01	15.67	0.5976	8.25	8.81	0.6668
5,000	19.31	17.99	0.6784	22.44	23.01	0.6940	12.91	12.92	0.6372
8,000	21.53	20.84	0.7266	25.46	27.08	0.7259	14.62	15.28	0.6153
10,000	23.33	22.86	0.7528	29.78	29.73	0.7477	16.15	16.74	0.6031
20,000	26.26	24.27	0.8136	33.71	35.40	0.8306	16.92	19.61	0.6678
30,000	27.22	25.11	0.8609	35.33	35.97	0.8909	18.92	21.80	0.7602
40,000	28.13	24.99	0.8968	36.48	36.95	0.9201	19.16	21.90	0.8196
50,000	28.88	25.78	0.9204	36.34	37.22	0.9397	18.78	22.34	0.8568
60,000	29.75	26.66	0.9382	36.57	37.37	0.9510	19.57	23.03	0.8846
70,000	29.80	<b>26.89</b>	0.9521	<b>37.59</b>	37.94	0.9642	19.91	22.95	0.9042
80,000	<b>30.01</b>	26.67	0.9609	36.89	38.06	0.9687	19.82	23.29	0.9144
100,000	29.99	26.52	0.9615	37.11	<b>38.09</b>	0.9622	20.51	23.94	0.9372
110,000	29.91	26.63	0.9648	37.10	38.15	0.9649	20.91	24.48	0.9578
120,000	29.86	26.58	0.9657	37.09	38.07	0.9680	20.92	24.40	0.9630
130,000	29.77	26.67	0.9625	37.29	38.03	0.9674	<b>21.21</b>	<b>24.69</b>	0.9596
140,000	29.69	26.62	0.9613	37.01	37.90	0.9636	21.00	24.52	0.9585

Table 4: BLEU scores of models with different vocabulary sizes on the En-De, En-Fr, and En-Zh translation tasks. Each configuration is averaged over three random seeds.

## A BPE algorithm

This shows a detailed description of BPE algorithm.

---

### Algorithm 1 Byte Pair Encoding (BPE)

---

**Require:** Corpus  $D$ , target vocabulary size  $V$

**Ensure:** Vocabulary set  $\mathcal{V}$

- 1: Initialize  $\mathcal{V}$  with all unique characters in  $D$
  - 2: Compute frequency of all adjacent symbol pairs in  $D$
  - 3: **while**  $|\mathcal{V}| < V$  **do**      $\triangleright$  Continue until target vocabulary size is reached
  - 4:     Identify the most frequent pair  $(s_i, s_j)$  in  $D$
  - 5:     Merge  $(s_i, s_j)$  into a new symbol  $s_k$
  - 6:      $\mathcal{V} \leftarrow \mathcal{V} \cup \{s_k\}$
  - 7:     Update  $D$  by replacing all occurrences of  $(s_i, s_j)$  with  $s_k$
  - 8:     Update frequencies of adjacent symbol pairs in  $D$
  - 9: **end while**
  - 10: **return**  $\mathcal{V}$
- 

## B Result for Translation Task

To investigate how vocabulary size affects machine translation performance, we conduct experiments on three language pairs (German-English, French-English, and Chinese-English). Each model variant is fine-tuned three times with different random seeds, and the average BLEU score is reported in Table 4

## C License and Terms of Use

We provide here the license information and terms of use for all datasets, models, and other artifacts used or created in this work.

### Pre-training Datasets.

- **OpenWebText** and **BookCorpus** were used to pre-train BERT in the NLP domain. OpenWebText is a publicly available dataset intended to replicate the quality of OpenAI’s WebText corpus and is distributed under an open research license.<sup>1</sup> BookCorpus was originally collected by [Zhu et al. \(2015\)](#) and is available for academic use only.
- **WMT16/17/18** datasets are used for multilingual pre-training and translation fine-tuning with mBART. These datasets are publicly released as part of the WMT shared tasks, licensed for research use.<sup>2</sup>
- **ZINC20** is used for pre-training in the chemistry domain. ZINC is a free database of commercially-available compounds provided by the Irwin and Shoichet Laboratories at UCSF. It is available for academic research under a public domain dedication (CC0).<sup>3</sup>
- **DNA sequences** used for genomics tasks are derived from public genome datasets and follow the same data sources as DNABERT2

<sup>1</sup><https://skylion007.github.io/OpenWebTextCorpus/>

<sup>2</sup><http://www.statmt.org/wmt16/>

<sup>3</sup><https://zinc20.docking.org/>

(Zhou et al., 2024). These datasets are in the public domain and used solely for academic research.

### Downstream Task Datasets.

- **GLUE Benchmark** datasets (Wang et al., 2018) are publicly released for research use and are commonly used under their respective licenses.
- **IWSLT14/15/17** datasets used for fine-tuning translation tasks are distributed for non-commercial research use as part of the IWSLT shared tasks.
- **MoleculeNet** datasets (e.g., BBBP, Tox21, Sider, ClinTox, HIV, BACE) are released under the MIT license and made publicly available by DeepChem.<sup>4</sup>
- **GUE Dataset** used for genomics classification tasks is adopted following the usage in DNABERT2 (Zhou et al., 2024), and is used for research purposes.

**Code and Models.** Our tokenizer construction scripts, Zipfian analysis tools, and vocabulary selection framework will be released under the MIT license. Any pre-trained models provided as part of this work will be licensed for academic research use only.

## D Experimental Details

**Computational Resources.** All experiments were conducted using a combination of 8 NVIDIA 2080Ti GPUs and 4 NVIDIA A10 GPUs. In total, our experiments consumed approximately 4,900 GPU-hours on 2080Ti and 2,400 GPU-hours on A10 cards. These computations include all pre-training, fine-tuning, hyperparameter search, and validation runs across all domains.

**Model Sizes.** The number of parameters used in each experimental setting is summarized below:

- **NLP (BERT models):** 84M to 124M parameters depending on vocabulary size.
- **NLP (mBART models):** 177M to 320M parameters depending on vocabulary size.
- **Genomics (BERT-based):** 80M to 93M parameters depending on vocabulary size.

- **Chemistry (BERT-based):** 72M to 90M parameters depending on vocabulary size.

**Reproducibility.** Each experiment was repeated using 3 different random seeds, and all reported results are averages over these runs.

**Software and Libraries.** We implemented all models using the HuggingFace Transformers library (v4.38) and PyTorch (v2.0). Data loading and pre-processing were done using the HuggingFace Datasets library. Evaluation metrics such as BLEU and ROC-AUC were computed using nltk, scikit-learn, and custom scripts, with standard configurations unless otherwise specified.

<sup>4</sup><https://moleculenet.org/>